Journal of Solution Chemistry, Vol. 35, No. 1, January 2006 (© 2006)
DOI: 10.1007/s10953-006-8940-5

Complexation and Precipitation of Arsenate and Iron Species in Sodium Perchlorate Solutions at 25 °C

Juan C. Raposo,[1,*] **María A. Olazábal,**[1]
and Juan M. Madariaga[1]

Received June 9, 2005; accepted July 27, 2005

The complexation of As(V) in aqueous solutions in the presence of iron(III) was investigated spectrophotometrically with both variable and constant ionic strengths. The determined thermodynamic and stoichiometric formation constants of the $FeHAsO_4^+$ species are $\log_{10} {}^{\circ}\beta = 9.21 \pm 0.01$ and $\log_{10} {}^{I}\beta$ ($1.0\,mol{\cdot}dm^{-3}$ $NaClO_4$) $= 7.78 \pm 0.01$, respectively. The numerical treatment of the obtained spectral data was performed with the SPECA program. The analysis required the consideration of the hydrolysis of Fe(III) and the protonation of As(V) in the pH range studied. No significant hydrolysis was observed because of the low pH values ($pH < 2.5$) involved. The stabilities of the solid Fe(III) arsenates was established by solubility experiments. All of the solubility experiments were performed in aqueous $NaClO_4$ solutions at constant ionic strength ($1.0\,mol{\cdot}dm^{-3}$) and at 25 °C. The experimental data were consistent with $FeAsO_4{\cdot}2H_2O$ being the solid phase ($\log_{10} {}^{\circ}K_{so} = -24.30 \pm 0.08$). The corresponding thermodynamic constants were computed by means of the Modified Bromley's Methodology (MBM) that describes the variation of the activity coefficients of all of the ions involved in the complexation and precipitation equilibria with the medium and ionic strength. Finally, the solid phase obtained in this work was also characterized by FT-IR and FT-Raman spectroscopies, and the hydration of the solid iron arsenate was confirmed by X-ray diffraction data.

KEY WORDS: Iron(III) arsenate; complexation equilibria; precipitation equilibria; thermodynamic model; spectroscopic characterization.

1. INTRODUCTION

One of the main factors controlling the concentration of inorganic arsenic in natural aquatic systems is the presence of ligands in the sediments that react with soluble arsenate species by means of precipitation or complexation reactions.

---

[1] Department of Analytical Chemistry, University of the Basque Country, 644 PK, E-48080, Bilbao, Spain; e-mail: qabrafej@lg.ehu.es

Along this line, some authors have emphasized that the adsorption and mobility processes of the arsenate anion into/from natural sediments is mainly controlled by the amount of the iron(III) oxides in the solid phases.(1−4)

Furthermore, a better knowledge of arsenic immobilization mechanisms in natural systems is necessary to develop and to implement removal or protection processes. To achieve this, different processes such as reverse osmosis, coagulation and filtration, or precipitation with soluble iron(III) salts should be implemented in the treatment plants. For the control of arsenate mobility or adsorption by iron(III), and the implementation of removal processes for the inorganic arsenic, it is important to be able to model the interactions of the primary form of arsenic (arsenate) with iron(III), and to define how those interactions are affected by changes in the composition of the medium or ionic strength of the natural waters.

Published information indicates that $FeAsO_4(s)$(5−7) is the main solid phase that controls the solubility of arsenate in natural waters. In 1996 Leblanc(8) described the formation of some amorphous ferric arsenates in aqueous solutions. However, there were no data reported for the variation of the precipitation constant with ionic strength and the solubility information was reported as the solubility product at infinite dilution (thermodynamic solubility product).

Therefore, it is necessary to perform solubility experiments at different ionic strengths in order to characterize the corresponding ferric arsenates as a function of the medium composition and to determine the variation of the precipitation constant with ionic strength. Then, the stoichiometric solubility constant obtained experimentally for a given ionic medium, *e.g.*, $NaClO_4$, can be extrapolated to infinite dilution by using the Modified Bromley's Methodology (MBM).(9,10)

In order to perform a correct extrapolation and interpretation of the solubility data, all other possible equilibria affecting both Fe(III) and As(V) in solution (hydrolysis and/or complexation) need to be considered. For this purpose, the chemical models of Fe(III)(11) and As(V)(12) can be used. These chemical models, constructed by means of the MBM, define all of the interaction parameters of Fe(III) and As(V) with the ions of the considered ionic medium, along with the corresponding thermodynamic constants for the hydrolysis of the Fe^{3+} cation and the protonation constants of the AsO_4^{3-} anion, respectively. Thus, the only reactions to be studied, besides the solubility experiments, are the formation of iron(III) arsenate complexes.

In this work, the complex formation equilibrium between As(V) and Fe(III) was studied by UV-vis spectrometry as suggested in the literature(13) and the precipitation equilibrium between As(V) and Fe(III) was studied through solubility experiments. For both types of measurements, the experiments were performed in $NaClO_4$ solutions of constant strength. The solubility study falls into three clearly different parts: (a) preparation of the solid iron arsenate, (b) the determination of its stoichiometry, and (c) the calculation of the solubility products for the precipitate. Moreover, the spectroscopic characterization of the precipitated iron arsenate was carried out by means of FT-IR and FT-Raman spectroscopies, along with an X-ray diffraction study.

2. EXPERIMENTAL

2.1. Reagents and Solutions

The chemicals used in the experiments were all of analytical reragent grade, with purities >99%. All solutions were prepared in freshly purified Milli-Q water.

Sodium arsenate (Aldrich, p.a.) stock solutions were standardized by acid-base titrations using bromocresol green as the indicator.(14) Ferric nitrate (Merck, p.a.) stock solutions were standardized by titration with EDTA (Panreac, p.a.) with 5-sulphosalicilic acid as indicator.(14)

The ionic medium was sodium perchlorate (Fluka, p.a.), whose concentrations were determined gravimetrically after evaporation of aliquots of the stock solutions and drying at 110 °C.

Stock solutions of perchloric acid (Fluka, puriss, p.a.) were also used and their concentrations were standardized against tris(hydroxymethyl)aminomethane (Merck, p.a.) using bromocresol green as the indicator.(15)

2.2. Experimental Procedure

For the complexation studies, solutions were prepared with different Fe(III) (0.001 and 0.0005 $\text{mol}\cdot\text{dm}^{-3}$) and As(V) (0.0001, 0.0005, and 0.00029 $\text{mol}\cdot\text{dm}^{-3}$) concentrations. In addition, experiments were performed with solutions not containing Fe(III) but containing arsenate at the same concentrations mentioned above. The experiments were performed in both 1.0 $\text{mol}\cdot\text{dm}^{-3}$ $NaClO_4$ constant ionic medium and with variable ionic strength. The pH values were varied by the addition of $HClO_4$ at the same ionic strength. The solutions were equilibrated in an oil bath thermostat at 25 °C for 1 week. After that, the pH value was measured and the UV-vis spectrum was obtained with a diode array spectrophotometer (Hewlett Packard 8452A).

The solubility experiments were performed by generating the precipitates at a constant concentration of both iron and arsenate ions (1/1 ratio at 0.014 $\text{mol}\cdot\text{dm}^{-3}$). The experiments were performed in 1.0 $\text{mol}\cdot\text{dm}^{-3}$ $NaClO_4$ ionic medium and the pH was controlled by adding $HClO_4$ at the same ionic strength. In all cases, the solutions were mixed with stirring to avoid local precipitate formation and the temperature was controlled at 25 °C in a thermostatted oil bath. In order to determine when equilibrium was reached, the pH of the saturated solutions was measured periodically until constant values were obtained (Crison micropH 2000). The concentrations of As and Fe in the saturated solutions equilibrated with the solid phases were measured by ICP-AES (ARL Fisons 3410).

The spectroscopic studies were made using a FT-IR spectrometer (Nicolet Nexus), a FT-Raman spectrometer (Nicolet 950) and a Rx diffractometer (Philips PW 1710). After separation from the equilibrated saturated solutions, the precipitates were washed with water several times to eliminate any traces of $NaClO_4$ (from the ionic medium), Na^+ (from the arsenate reagent) and NO_3^- (from the Fe(III) salt). The precipitates were dried in vacuum for one week. Finally, each precipitate was stored in a desiccator prior to the spectroscopic analyses.

3. RESULTS AND CALCULATIONS

3.1. Spectrophotometric Experimentation

In all of the experiments, the E° values of the electrolytic cell were determined using Gran's method,(16) by means of titrations with $HClO_4$ in the corresponding ionic medium and ionic strength ($1.0\,\text{mol}\cdot\text{dm}^{-3}$ $NaClO_4$). The Nernst equation(17) was then used to calculate the pH values, defined as $-\log_{10}[H^+]$, in all of the solutions. The free concentration of hydrogen ions (H^+) was calculated from the measured E by using equations:

$$E = E^\circ + 59.16\ \log_{10}[H^+] + E_{j,h} \tag{1}$$

and

$$E_{j,h} = j_{ac}[H^+] + j_{bas}K_W[H^+]^{-1} \tag{2}$$

where j_{ac} and j_{bas} are the acidic and the basic solution liquid junction potential coefficients, respectively, and K_W is the autoprotolysis constant of water for the ionic medium at the given ionic strength. All of these parameters were determined at the given ionic strength by means of separate potentiometric titrations in the ionic medium. They were calculated using Gran's method and refined numerically with the Model Function(18) version of the Letagrop program.(19) Because the equation used to calculate the h value can not be solved analytically, an iterative procedure, the Newton–Raphson method,(17) was used by implementing it in an Excel® spread sheet.(20)

A numerical analysis of absorbtivity *versus* pH for each dataset was performed by means of the SPECA program,(21) in order to determine both the thermodynamic (from the experiments without constant ionic medium) and stoichiometric constants (from the experiments in $NaClO_4$ ionic media). In addition, the absorbitivity coefficients of all species involved in the complexation equilibrium were calculated using the SPECA program.

The isosbestic point ($\lambda = 270\,\text{nm}$), characteristic of the Fe^{3+} spectra (Fig. 1a), disappeared upon the addition of arsenate to the solution (Fig. 1b). This observation can only be explained by the formation of iron arsenate complexes. In order to determine the wavelengths containing the most important spectral information, a

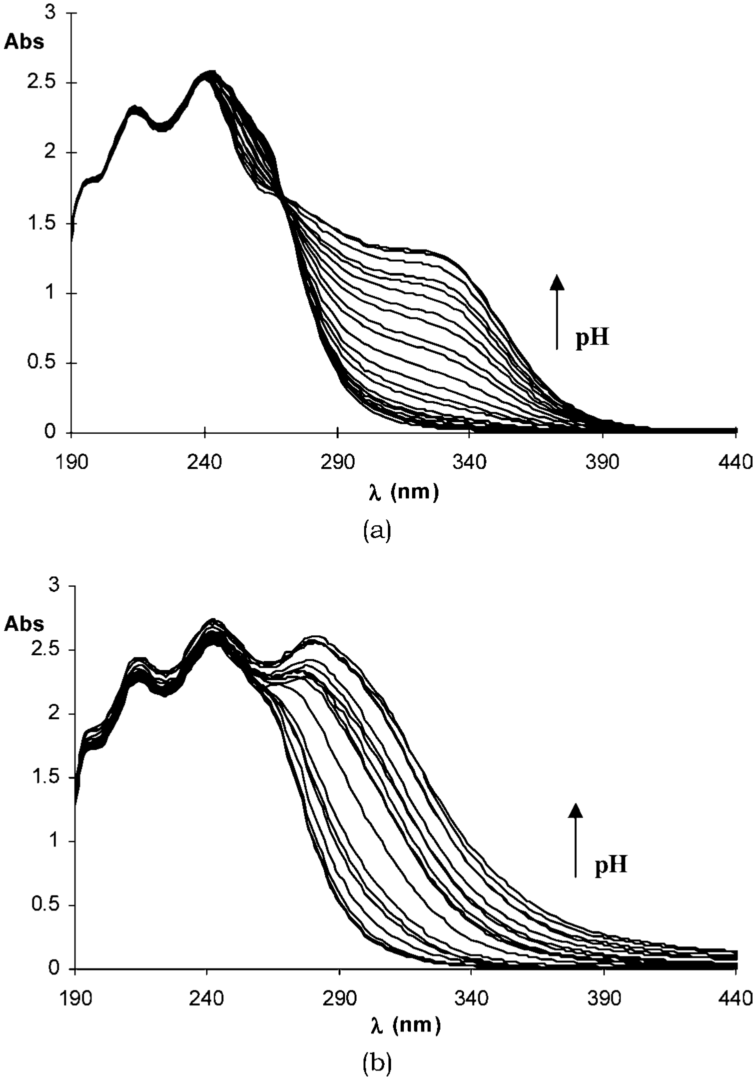

Fig. 1. Variation of the (a) Fe(III) (0.001 mol·dm^{-3}) and (b) Fe(III) (0.001 mol·dm^{-3}) + $HAsO_4^{2-}$ (0.0005 mol·dm^{-3}) spectra with pH (0.9 < pH < 2.2).

computer routine in MATLAB 4.0$^{(22)}$ was created in our laboratory. The results obtained indicate that 290, 300 and 310 nm were the most important wavelengths. Prior to the numerical treatment, it was verified that there were no spectral features due to the $NaClO_4$, $HClO_4$ and $HAsO_4^{2-}$ species in the wavelength range of interest.

Table I. Absorbtivity Coefficients and Thermodynamic and Stoichiometric Formation Constants of the Soluble $FeHAsO_4^+$ Complex at 25 °C

	$I \rightarrow 0$	$1.0\,mol{\cdot}dm^{-3}$
$\log_{10}\beta$	9.21 ± 0.01	7.78 ± 0.01
ε_{290}	3888 ± 25	5771 ± 14
ε_{300}	3075 ± 22	4707 ± 16
ε_{310}	2180 ± 17	3414 ± 11

The fittings of the absorbtivity *versus* pH data were performed assuming the presence of only Fe^{+3} and $Fe(OH)^{2+}$ species for Fe(III)[11,23] and the protonated forms of the arsenate anion.(12) Several possible chemical models with different assumed iron arsenate complexes were examined by the SPECA program. The results show that only one arsenate complex is present in the solutions, $FeHAsO_4^+$, whose formation equilibrium can be expressed as

$$Fe^{3+} + HAsO_4^{2-} \longleftrightarrow FeHAsO_4^+ \tag{3}$$

This equilibrium reaction is adequate to explain the whole set of spectrometric data with a global standard deviation of $\sigma(A) = \pm 0.005$.

The stoichiometric and thermodynamic constants of equilibrium (1) and the absorbitivity coefficient of the new complex computed by SPECA are summarized in Table I. As examples, Figs. 2 and 3 show the fittings obtained from the numerical treatment.

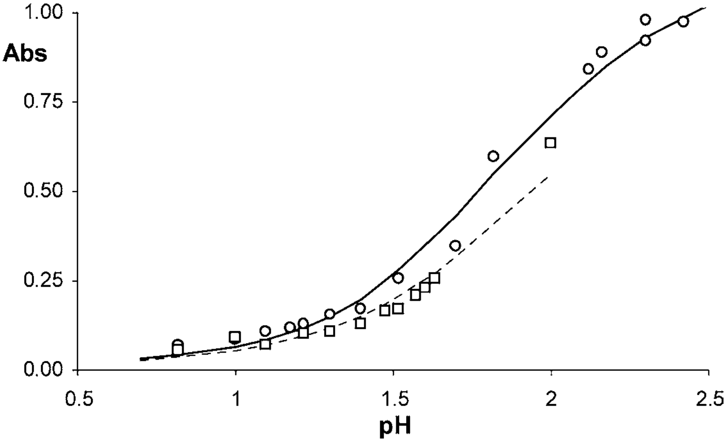

Fig. 2. Variation of the absorbtivity *versus* pH data in solutions with an Fe^{3+} concentration of $0.0005\,mol{\cdot}dm^{-3}$ and AsO_4^{3-} concentrations of 0.001 (○–○) or 0.0005 (□ –□) $mol{\cdot}dm^{-3}$ at 310 nm.

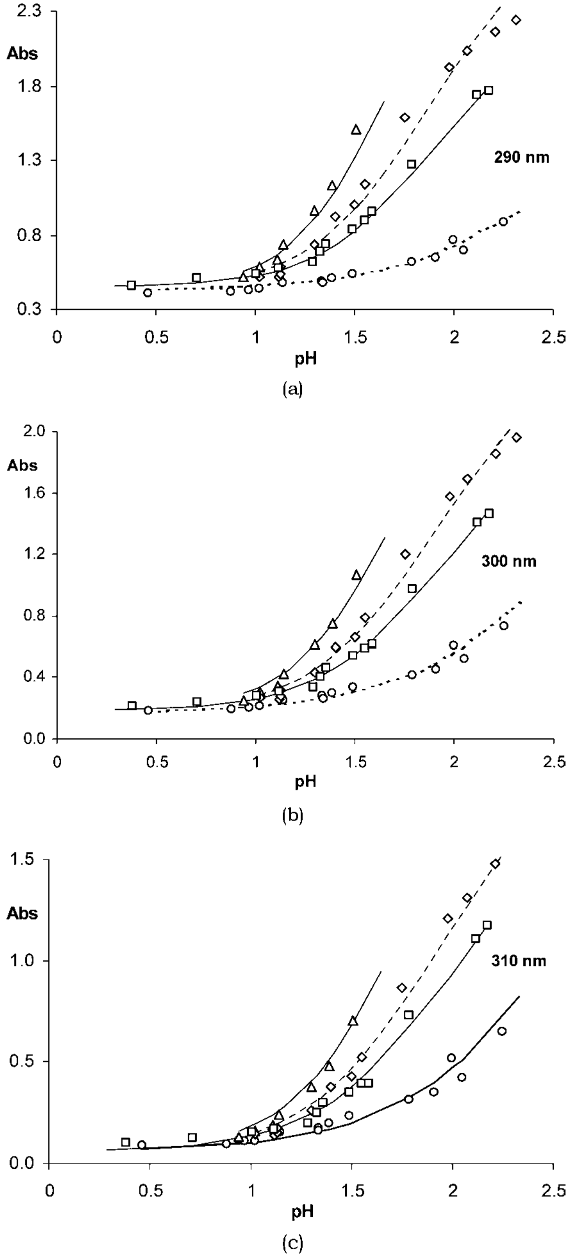

Fig. 3. Variation of the absorbtivity *versus* pH data in solutions with an Fe^{3+} concentration of 0.001 mol·dm^{-3} (○–○) and AsO$_4^{3-}$ concentrations of 0.001 (Δ–Δ), 0.0005 (◇–◇) and 0.00029 (□–□) mol·dm^{-3} in 1.0 mol·dm^{-3} $\mathrm{NaClO_4}$.

Table II. Raw Data (Solution Concentrations) Obtained in the Solubility Experiments

pH	C_{Fe} (mol·dm^{-3})	C_{As} (mol·dm^{-3})
0.98	0.00772	0.00982
1.15	0.00450	0.00599
1.26	0.00151	0.00225
1.36	0.00072	0.00123
1.45	0.00043	0.00089
1.49	0.00038	0.00089
1.56	0.00026	0.00080
1.64	0.00021	0.00077
1.68	0.00013	0.00071
1.73	9.5×10^{-5}	0.00051
1.80	8.2×10^{-5}	0.00060
1.82	9.7×10^{-5}	0.00062
1.85	6.9×10^{-5}	0.00061
1.91	4.7×10^{-5}	0.00058
1.95	4.5×10^{-5}	0.00061
1.99	4.0×10^{-5}	0.00064
2.17	1.5×10^{-5}	0.00497
2.83	3.1×10^{-6}	0.00080
7.75	2.3×10^{-6}	0.00303
12.33	2.0×10^{-6}	0.01050

3.2. Solubility Data

The raw solubility data are listed in Table II. The concentration profiles obtained in the solubility experiments imply the presence of solid iron arsenate, since there was a simultaneous decrease of the concentrations of both the arsenate and metal in the range of $1 < \mathrm{pH} < 2.5$ (Fig. 4). For $\mathrm{pH} > 2.5$, the concentration profiles were explained by the formation of a $\mathrm{Fe(OH)_3(s)}$ precipitate with the liberation of arsenate anion to the solution phase. As it can be seen in Fig. 4, the concentration profile of the total arsenate concentration did not show the theoretical redissolution behavior. This fact can be explained by the well-known adsorption of the arsenate anion on the precipitated $\mathrm{Fe(OH)_3(s)}$.(1–4)

The formation of the new precipitate can be described by the general equilibrium:

$$p\mathrm{Fe}^{3+} + q\mathrm{H}^{+} + r\mathrm{AsO}_4^{3-} \longleftrightarrow (\mathrm{Fe}^{3+})_p \cdot (\mathrm{H}^{+})_q \cdot (\mathrm{AsO}_4^{3-})_r(s) \qquad (4)$$

with the corresponding stoichiometric solubility product:

$$K_{s0}^{I} = [\mathrm{Fe}^{3+}]^p \cdot [\mathrm{H}^{+}]^q \cdot [\mathrm{AsO}_4^{3-}]^r \qquad (5)$$

where [] denotes the molar concentrations of the species involved in the precipitation equilibrium.

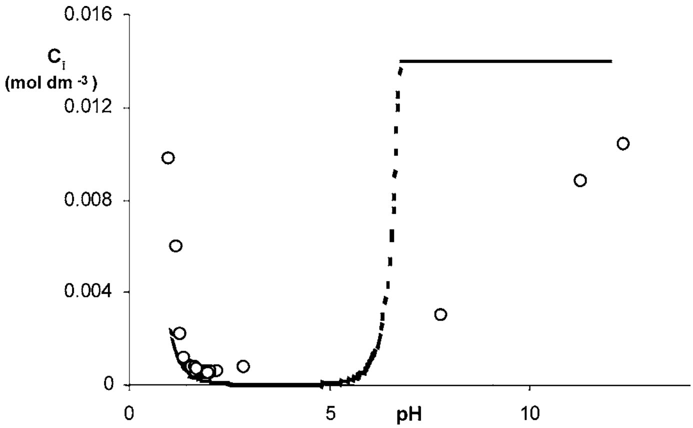

Fig. 4. Variation of the total concentration As(V) in solution. The predicted solubility of As(V) in 1.0 mol·dm^{-3} $NaClO_4$ is also shown. The (—) line is the theoretical solubility profile for As(V) without adsorption occurring.

The values of $[H^+]$ were calculated from the experimental pH values. The free $[AsO_4^{3-}]$ and $[Fe^{3+}]$ concentrations were obtained from the mass-balance equations by using the experimental total concentrations of As(V) and Fe(III), the pH value for each solution, and the chemical model for the soluble species: Fe^{3+}, $Fe(OH)^{2+}$, $FeHAsO_4^+$, H_3AsO_4, $H_2AsO_4^-$, $HAsO_4^{2-}$, and AsO_4^{3-} at 1.0 mol·dm^{-3} $NaClO_4$ ionic strength. Using these data, a graphical treatment was performed by considering the relationship between the concentrations of the AsO_4^{3-} and H^+ species on one hand and between Fe^{3+} and H^+ on the other. The reaction stoichiometries $(p{:}q{:}r)$ can be determined from the slopes of the different straight lines plotted in Fig. 5a and b.

Because neither the $[Fe^{3+}]$ nor the $[AsO_4^{3-}]$ had constant values at any pH value, the saturation condition (5) could be extended to the following three equations:

$$K_{s0}^{I} = (cte_2)(cte_1) = [Fe^{3+}]^p \cdot [H^+]^{(q_1+q_2)} \cdot [AsO_4^{3-}]^r \qquad (6)$$

with

$$cte_2 = [Fe^{3+}]^p \cdot [H^+]^{q_1} \qquad (7)$$

and

$$cte_1 = [H^+]^{q_2} \cdot [AsO_4^{3-}]^r \qquad (8)$$

Moreover, the electroneutrality condition for any solid phase requires that

$$2p + q = 3r \qquad (9)$$

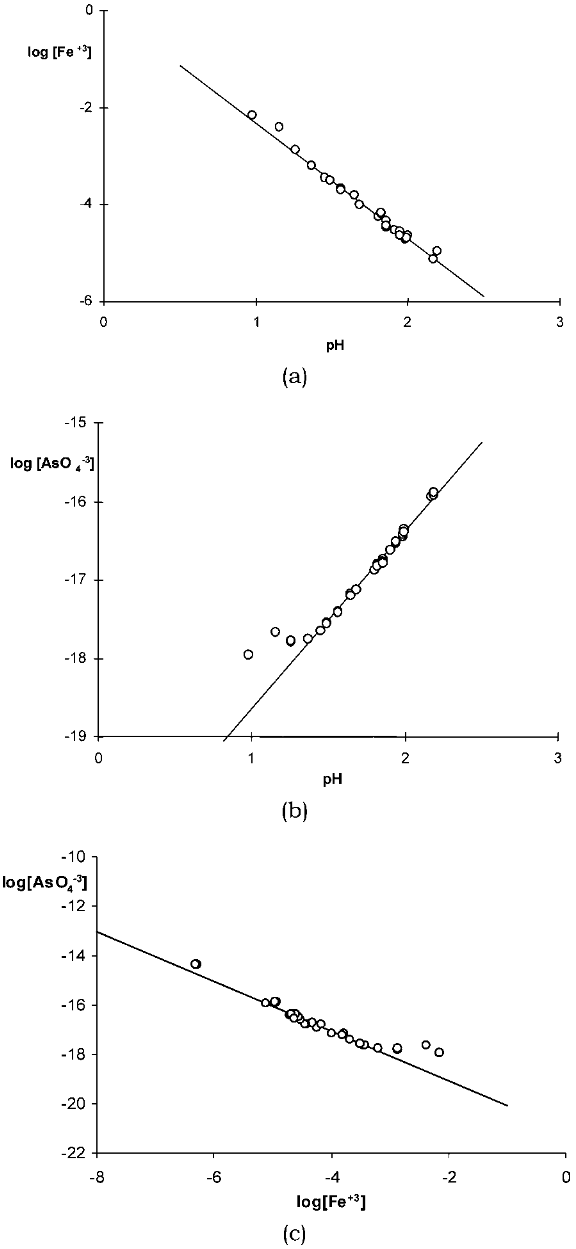

Fig. 5. Plot of $\log_{10} C_i$ *versus* pH for the free concentrations of (a) Fe^{3+} and (b) AsO_4^{3-} species; and (c) plot of $\log_{10} C_{\mathrm{arsenate}}$ *versus* $\log_{10} C_{\mathrm{iron}}$ for the free concentrations (—, theoretical line with slope = 1.0).

with

$$q = q_1 + q_2 \tag{10}$$

Applying condition (7) to Fig. 5a, the slope of this plot (= −2.2) gives the value of the ratio q_1/p. In the same way, condition (8) gives the value of the ratio q_2/r for the slope (= 2.2) of Fig. 5b and, taking into account Eqs. (9) and (10), the following indexes were obtained: $p = 1, q = 0$ ($q_1 = -2.2, q_2 = 2.2$) and $r = 1$. In other words, $FeAsO_4$(s) is the composition obtained for the solid phase at pH < 2.5.

From the previously calculated $[H^+]$, $[AsO_4^{3-}]$ and $[Fe^{3+}]$ concentrations, the stoichiometric solubility constant of the precipitate was calculated at each experimental point (see Fig. 6) using Eq. (5). The obtained value for the stoichiometric solubility product of $FeAsO_4$(s) is $\log_{10} {}^I K_{s0} = -21.08 \pm 0.07$ (in 1.0 mol·dm^{-3} $NaClO_4$ at 25 °C). Figure 6 shows that there is no systematic drift in the $\log_{10} {}^I K_{so}$ values for the whole investigated pH range.

4. DISCUSSION

The presence of hydration waters in the precipitated $FeAsO_4 \cdot xH_2O$(s) was confirmed by the characteristic signals of H—O—H in the spectral regions 3560 to 3400 cm^{-1} and 1650 to 1600 cm^{-1}, which were obtained from the IR spectra (see Table III). The value of "x" in the precipitate was obtained in this work by comparison of the data obtained from X-ray diffraction with those reported in the literature. In that manner, the formulation of $FeAsO_4 \cdot 2H_2O$ was established.

Inasmuch as this solid was obtained by mixing Na_2HAsO_4 and $Fe(NO_3)_3$ salts, the IR signals of $Na_2HAsO_4 \cdot 7H_2O$ are also reported in Table III for the

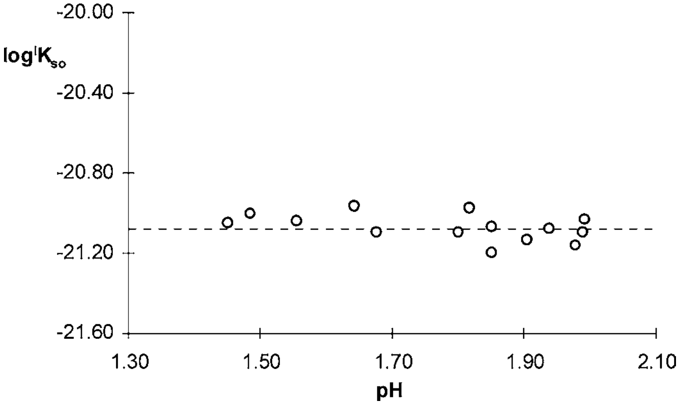

Fig. 6. Stoichiometric solubility product of $FeAsO_4$ obtained from the solubility experiments.

Table III. FT-IR Spectra (cm^{-1}) Obtained for Iron Arsenate Precipitates Compared to Those from This Study

$FeAsO_4 \cdot 2H_2O$		$Na_2HAsO_4 \cdot 7H_2O$[a]	AsO_4^{3-}[b]	Assignment
3545				H—O—H stretching
3467		344.3		H—O—H stretching
3404		335.9		H—O—H stretching
1641		168.8		H—O—H bending
1618		162.9		H—O—H bending
		859	878	(ν_3) AsO_4^{3-}
836	840[a]	833	837	(ν_1) AsO_4^{3-}
470	472[a]		463	(ν_4) AsO_4^{3-}

[a] From Miller.(24)
[b] From Nakamoto.(23)

purpose of confirming that disodium arsenate was absent from the solid phase. The reported frequencies for dissolved AsO_4^{3-} are also known.(24) The H—O—H stretching bands are well defined for the hydrated arsenate ion, as are the two H—O—H bending signals. These five frequencies are different from those found experimentally for $Na_2HAsO_4 \cdot 7H_2O$. Two different characteristic arsenate bands occurring at 836 cm^{-1} (ν_1) and 470 cm^{-1} (ν_4) were observed for the iron arsenate obtained in this work; the frequencies for the two bands are in good agreement with those reported by Miller.(25) However, the band around 590 cm^{-1} found for $Na_2HAsO_4 \cdot 7H_2O$ (594 cm^{-1}) by Miller(25) was not observed by us. Also, the ν_3 band of arsenate was not observed.

Three As—O—H wagging signals were obtained in the Raman spectrum (Table IV) using the 1064 cm^{-1} laser as the excitation source. In the Raman spectrum, the ν_3 band is well defined (it is not seen in the IR one) but ν_1 did not appear. The ν_4 vibration band was split into two very sharp bands (482 and 444 cm^{-1}). Also, a split As—O—H rocking band was obtained at 655 and

Table IV. Raman Spectra (cm^{-1}) Obtained Here for the Iron Arsenate Precipitate

$FeAsO_4 \cdot 2H_2O$	Assignment
1146	As—O—H wagging
1097	As—O—H wagging
1088	As—O—H wagging
888	(ν_3) AsO_4^{3-}
655	As—O—H rocking
620	As—O—H rocking
482	(ν_4) AsO_4^{3-}
444	(ν_4) AsO_4^{3-}

620 $\mathrm{cm^{-1}}$. These arsenate frequencies are similar to those obtained in a previous work for the calcium and magnesium arsenates.(26)

The thermodynamic solubility constant was calculated using the relationship with the stoichiometric solubility products, obtained experimentally, and the corresponding activity coefficients:

$$\log_{10} K^{I}_{s0} = \log_{10} K^{\circ}_{s0} - \log_{10} \gamma_{\mathrm{Fe^{3+}}} - \log_{10} \gamma_{\mathrm{AsO_4^{3-}}} \tag{11}$$

The values of γ_X were estimated by using the MBM expression on the molar composition scale:

$$\log_{10} \gamma_X = \frac{-A_c |Z_X|^2 I^{1/2}}{1 + I^{1/2}} + \left(\frac{(0.06 + 0.6 B_{YX}) |Z_Y Z_X|}{\left(1 + \frac{1.5}{|Z_Y Z_X|} I\right)^2} + B_{YX} \right) \frac{(|Z_Y| + |Z_X|)^2}{4} I \tag{12}$$

where I is the ionic strength on the molar scale and B_{YX} is the ionic interaction parameter of species X ($\mathrm{AsO_4^{3-}}$ or $\mathrm{Fe^{3+}}$) involved in the precipitation equilibrium with the Y ions in the ionic medium ($\mathrm{Na^+}$ or $\mathrm{ClO_4^-}$). The B_{YX} values in the $\mathrm{NaClO_4}$ ionic medium for $\mathrm{Fe^{3+}}$ (11) and $\mathrm{AsO_4^{3-}}$ (12) were determined previously. Therefore, the only unknown parameter, the thermodynamic solubility product, was calculated using Eqs. (11) and (12) and found to be $\log_{10}{}^{\circ}K_{s0} = -24.30 \pm 0.08$.

In the same way, it was possible to estimate the ionic interaction parameter of $\mathrm{FeHAsO_4^+}$ with $\mathrm{ClO_4^-}$ using Eq. (12) and the MBM to calculate the activity coefficients of the following expression:

$$\log_{10} {}^{I}\beta = \log_{10} {}^{\mathrm{o}}\beta + \log_{10} \gamma_{\mathrm{Fe^{3+}}} + \log_{10} \gamma_{\mathrm{HAsO_4^{2-}}} - \log_{10} \gamma_{\mathrm{FeHAsO_4^{+}}} \tag{13}$$

This equation relates the values of the stoichiometric and thermodynamic formation constants reported in Table I.

The ionic interaction parameter was evaluated by direct calculation using Eq. (13): $B_{\mathrm{FeHAsO_4^+}} = -0.4814 \pm 0.0009$ on the molar scale.

Finally, the influence of the ionic medium on the distribution of the iron and arsenate ions was examined. For this purpose, the MEDUSA program(27) was used to calculate the concentrations of all of the soluble arsenic and iron species as well as of the Fe(III) precipitates. All the thermodynamic formation constants were extrapolated to various environmental conditions by using the MBM to calculate the activity coefficients for each particular medium and ionic strength.

The distribution of the stable Fe(III) species as a function of pH was calculated for river water ($I < 0.1\ \mathrm{mol{\cdot}dm^{-3}}$ as NaCl) and estuarine water ($I = 0.7\ \mathrm{mol{\cdot}dm^{-3}}$ as NaCl), for typical concentrations of iron and arsenic ions that are

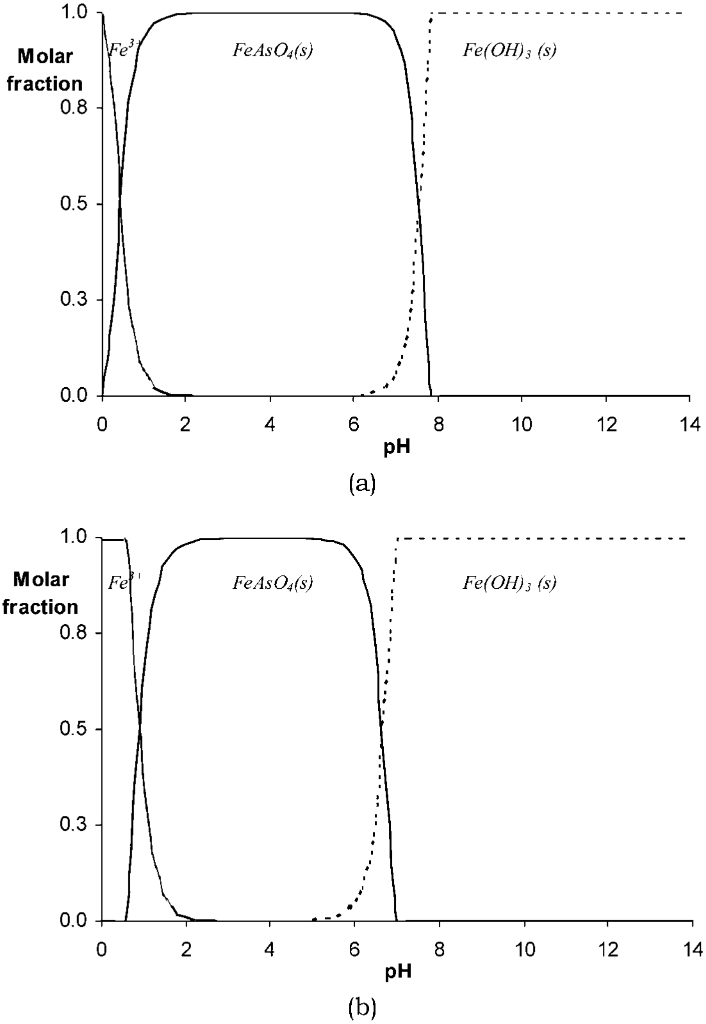

Fig. 7. Distribution diagram of Fe(III) as a function of pH at typical concentrations$^{(1)}$ (As(V) = 60 μg·L^{-1}, Fe(III) = 70 μg·L^{-1}) for river (a) and estuarine waters (b), considering the formation of $FeHAsO_4^+$, $Fe(OH)^{2+}$, $Fe(OH)_3(s)$ and $FeAsO_4(s)$.

found in natural systems. The respective species distribution diagrams are shown in Fig. 7a and b. As can be seen, the iron(III)-arsenate precipitate can form, depending on the pH as well as the composition of the ionic medium. It was found that the pH range for the predominance of $FeAsO_4$ is higher in river waters than in seawater, and that $FeHAsO_4^+$ is not a predominant species at least for [Fe(III)]/[As(V)] = 1 and at the pH range of most natural waters (7.0 to 8.5). The presence of Fe(III) could control the retention of As(V) as a solid phase in river waters, but this is less probable in estuarine waters and seawaters because $Fe(OH)_3(s)$ is more stable than the $FeAsO_4(s)$ under those conditions. For such waters with a relatively high ionic strength, the retention of As(V) in the $Fe(OH)_3(s)$ solid phase can be explained by adsorption processes (as showed in the experimental data ploted in Fig. 4b), rather than arsenate precipitation.

ACKNOWLEDGMENT

This work was performed as part of the project UPV EB130/99, whose financial support is gratefully acknowledged.

REFERENCES

1. M. L. Pierce and C. B. Moore, Adsorption of Arsenite and Arsenate on Amorphous Iron Hydroxide, *Water Res.* **16**, 1247–1253 (1982).
2. P. E. Mariner, F. J. Holzmer, R. E. Jackson, and H. W. Meinardus, Effects of High pH on Arsenic Mobility in a Shallow Sandy Aquifer and on Aquifer Permeability Along the Adjacent Shoreline, Commencement Bay Superfund Site, Tacoma, Washington, *Environ. Sci. Technol.* **30**, 1645–1651 (1996).
3. E. E. van der Hoek and R. N. J. Comans, Modelling Arsenic and Selenium Leaching from Acidic Fly Ash by Sorption on Iron(hydr)oxide in the Fly Ash Matrix, *Environ. Sci. Technol.* **30**, 517–523 (1996).
4. B. Daus, J. Mattusch, A. Paschke, H. Weiss, and R. Wennrich, Kinetics of the Arsenite Oxidation in Seepage Waters from a Tin Mill Tailings Pond, *Talanta* **51**, 1087–1095 (2000).
5. L. G. Sillen and A. E. Martell, *Stability Constants of Metal-Ion Complexes* (Metcalfe & Cooper Limited, London, 1964).
6. J. D. Rimstidt and P. M. Dove, Solubility and Stability of Scorodite, $FeAsO_4{\cdot}2H_2O$, *Am. Miner.* **72**, 852–855 (1987).
7. C. R. Paige, W. J. Snodgrass, R. V. Nicholson, and J. M. Scharer, An Arsenate Effect on Ferrihydrite Dissolution Kinetics under Acidic Oxic Conditions, *Water Res.* **31**, 2370–2382 (1997).
8. M. Leblanc, B. Achard, D. Othman, and J. M. Luck, Accumulation of Arsenic from Acidic Mine Waters by Ferruginous Bacterial Accretions (Stromatolites), *Appl. Geochem.* **11**, 541–554 (1996).
9. G. Borge, R. Castaño, M. P. Carril, M. S. Corbillón, and J. M. Madariaga, Development of a Modified Bromley's Methodology (MBM) for the Estimation of Ionic Media Effects on Solution Equilibria. Part 1. Calculation of the Interaction Parameters in the Molar and Molal Scales at 25 °C, *Fluid Phase Equil.* **121**, 85–98 (1996).
10. G. Borge, N. Etxebarria, L. A. Fernandez, M. A. Olazábal, and J. M. Madariaga, Development of a Modified Bromley's Methodology (MBM) for the Estimation of Ionic Media Effects on Solution Equilibria. Part 2. Correlation of the Molar and Molal Interaction Parameters with the Charge and Crystal Radii of the Ions, *Fluid Phase Equil.* **121**, 99–109 (1996).
11. Y. Belaustegui, *Elimination of Fe(III), Zn(II), Cu(II) and Cd(II) in Solutions with High HCl Concentrations by Ionic Exchange* (Ph.D Thesis, UPV/EHU, Leioa, Spain, 1995).
12. J. C. Raposo, J. Sanz, O. Zuloaga, M. A. Olazábal, and J. M. Madariaga, The Thermodynamic Model of Inorganic Arsenic Species in Aqueous Solutions. Potentiometric Study of the Hydrolytic Equilibrium of Arsenic Acid, *Talanta* **57**, 849–857 (2002).

13. G. H. Khoe and R. G. Robins, The Complexation of Iron(III) with Sulfate, Phosphate or Arsenate Ion Sodium Nitrate Medium at 25 °C, *J. Chem. Soc. Dalton Trans: Inorg. Chem.* **8**, 2015–2021 (1998).
14. E. Bishop, *Indicators* (Pergamon Press, Oxford, Great Britain, 1972).
15. G. H. Jeffery, J. Basset, J. Mendham, and R. C. Denney, *Vogel's Textbook of Quantitative Chemical Analysis* (6th de Longman, London, Great Britain, 2000).
16. G. Gran, Determination of the Final Point in the Potentiometric Titrations II, *Analyst* **77**, 661–671 (1952).
17. F. J. C. Rossotti and H. Rossotti, *The Determination of Stability Constants* (McGraw-Hill, New York, 1961, 127).
18. J. C. Raposo, J. Sanz, O. Zuloaga, M. A. Olazabal, and J. M. Madariaga, The Thermodynamic Model of Inorganic Arsenic Species in Aqueous Solutions. Potentiometric Study of the Hydrolytic Equilibrium of Arsenious Acid, *J. Solution Chem.* **32**, 253–264 (2003).
19. N. Ingri and L. G. Sillén, High Speed Computers as Supplement to Graphical Methods II. Some Computer Programs for Studies of Complex Formation Equilibria, *Acta Chem. Scand.* **16**, 173–191 (1962).
20. Excel 2000, Microsoft Corporation, Redmond. WA, 2001.
21. R. Cazallas, M. J. Citores, N. Etxebarria, L. A. Fernández, and J. M. Madariaga, SPECA a Program for the Calculation of Thermodynamic Equilibrium Constants from Spectrophotometric Data, *Talanta* **41**, 1637–1644 (1994).
22. J. Ferre and F. X. Rius, Equivalence Between Selectivity and Variance Inflation Factors in Multicomponent Analysis, *Quím. Anal.* **15**, 259–262 (1996).
23. C. F. Baes and R. E. Mesmer, *The Hydrolysis of Cations* (John Wiley & Sons, New York, USA, 1976).
24. K. Nakamoto, *Infrared Spectra of Inorganic and Coordination Compounds* (2nd Ed., John Wiley and Sons, New York, USA, 1963).
25. N. Miller and J. Wilkins, Infrared Spectra and Characteristic Frequencies of Inorganic Ions, *Anal. Chem.* **24**, 1253–1294 (1952).
26. J. C. Raposo, O. Zuloaga, M. A. Olazábal, and J. M. Madariaga, Study of the Precipitation Equilibria of Arsenate Anion with Calcium and Magnesium in Sodium Perchlorate at 25 °C, *Appl. Geochem.* **19**, 855–862 (2004).
27. I. Puigdomenech, *MEDUSA, Make Equilibrium Diagrams using Sophisticated Algorithms* (Department of Inorganic Chemistry, Royal Institute of Technology, S-100 44, Stockholm, Sweden, 1999).